Published online 15 June 2020

Nucleic Acids Research, 2020, Vol. 48, No. 13 ***7239–7251***
doi: 10.1093/nar/gkaa503

Full length RTEL1 is required for the elongation of the single-stranded telomeric overhang by telomerase

Aya Awad[1,†], Galina Glousker[1,†], Noa Lamm[1], Shadi Tawil[1], Noa Hourvitz[1], Riham Smoom[1], Patrick Revy[2] and Yehuda Tzfati[1,*]

[1]Department of Genetics, The Silberman Institute of Life Sciences, The Hebrew University of Jerusalem, Givat Ram, Jerusalem 91904, Israel and [2]INSERM UMR 1163, Laboratory of Genome Dynamics in the Immune System, Equipe Labellisée Ligue contre le Cancer and Paris Descartes-Sorbonne Paris Cité University, Imagine Institute, Paris, France

Received December 29, 2019; Revised May 29, 2020; Editorial Decision June 01, 2020; Accepted June 02, 2020

ABSTRACT

Telomeres cap the ends of eukaryotic chromosomes and distinguish them from broken DNA ends to suppress DNA damage response, cell cycle arrest and genomic instability. Telomeres are elongated by telomerase to compensate for incomplete replication and nuclease degradation and to extend the proliferation potential of germ and stem cells and most cancers. However, telomeres in somatic cells gradually shorten with age, ultimately leading to cellular senescence. Hoyeraal-Hreidarsson syndrome (HHS) is characterized by accelerated telomere shortening and diverse symptoms including bone marrow failure, immunodeficiency, and neurodevelopmental defects. HHS is caused by germline mutations in telomerase subunits, factors essential for its biogenesis and recruitment to telomeres, and in the helicase RTEL1. While diverse phenotypes were associated with RTEL1 deficiency, the telomeric role of RTEL1 affected in HHS is yet unknown. Inducible ectopic expression of wild-type RTEL1 in patient fibroblasts rescued the cells, enabled telomerase-dependent telomere elongation and suppressed the abnormal cellular phenotypes, while silencing its expression resulted in gradual telomere shortening. Our observations reveal an essential role of the RTEL1 C-terminus in facilitating telomerase action at the telomeric 3′ overhang. Thus, the common etiology for HHS is the compromised telomerase action, resulting in telomere shortening and reduced lifespan of telomerase positive cells.

INTRODUCTION

Telomeres, the protective structures of eukaryotic chromosome ends, are composed of short tandem DNA repeats (TTAGGG in vertebrates) bound by a protein complex termed shelterin (1). The longer G-rich strand forms a 3′ overhang at the telomere end, which can fold back to invade the internal part of the telomere and create a displacement loop termed telomere loop (t-loop). A specialized enzyme termed telomerase can add telomeric repeats to the 3′ overhang to compensate for losses caused by incomplete DNA replication and degradation. Telomerase is barely expressed in most human somatic tissues. Consequently, telomeres gradually shorten with cell division and eventually activate the canonical DNA damage response (DDR) and cause cell cycle arrest or cell death. Thus, telomere length controls cellular lifespan and provides a tumor-suppressing mechanism (2). Indeed, telomerase is activated in most cancers to maintain telomere length and enable unlimited cell proliferation. Paradoxically, however, DDR activation by short or otherwise dysfunctional telomeres can also activate DNA repair mechanisms, and thus increase genomic instability, accumulation of mutations and cancer development (2).

Dyskeratosis congenita (DC) and its severe form, Hoyeraal-Hreidarsson syndrome (HHS), are telomere biology diseases (TBD), also termed telomeropathies, caused by severe telomere shortening (reviewed in (3,4)). DC is characterized by diverse clinical symptoms mainly in highly proliferative tissues, such as the hematopoietic system and epithelial cells. Bone marrow failure is the main cause of mortality. In addition to the DC symptoms, HHS patients display immunodeficiency, brain developmental defects and mortality at an early age (4). HHS-causing mutations were found in the telomerase reverse transcriptase (TERT), in

*To whom correspondence should be addressed. Tel: +972 2 6584902; Fax: +972 2 6586975; Email: tzfati@mail.huji.ac.il
†The authors wish it to be known that, in their opinion, the first two authors should be regarded as Joint First Authors.
Present addresses:
Galina Glousker, Swiss Institute for Experimental Cancer Research, School of Life Sciences, Ecole Polytechnique Fédérale de Lausanne (EPFL), 1015 Lausanne, Switzerland.
Noa Lamm, Genome Integrity Unit, Children's Medical Research Institute, University of Sydney, Westmead, New South Wales 2145, Australia.

factors essential for the processing, assembly and stability of the telomerase ribonucleoprotein complex—dyskerin and PARN, and in the shelterin subunits essential for the recruitment of telomerase—TIN2 and TPP1. The common function of these proteins in telomerase action, suggests that accelerated telomere shortening is the main cause for the disease. In addition, germline mutations in the helicase Regulator of Telomere Elongation 1 (RTEL1) were identified to cause severe telomere shortening and HHS (5–9), raising the question whether RTEL1 is likewise essential for telomerase action at telomeres. Indeed, in mouse, mRtel1 was found as a dominant factor regulating telomere length and was suggested to facilitate telomere extension by telomerase in a yet unknown mechanism (10,11). However, RTEL1 was suggested to play multiple additional roles in telomeric, as well as non-telomeric, genome stability: It associates with the replisome through binding to proliferating cell nuclear antigen (PCNA) to facilitate both genome-wide and telomeric replication (12); it is recruited to the telomeres by TRF1 to resolve G4 quadruplexes and repress telomere fragility (13); it is recruited to telomeres by TRF2 in S phase to promote t-loop unwinding (14,15); it stabilizes long G-overhangs in cells overexpressing telomerase (16); and facilitates pre-U2 snRNA trafficking between the nucleus and cytoplasm (17). The observed consequences of RTEL1 deficiency vary dramatically as a function of cell type, differentiation status, telomerase expression and the type and position of the RTEL1 mutation. *Rtel1*$^{-/-}$ mouse embryos die between days 10 and 11.5 of gestation, and *Rtel1*$^{-/-}$ embryonic stem (ES) cells show rapid increase in genomic instability and cell death upon induction of differentiation (11). Failure to resolve t-loops was found in some cell types deficient for RTEL1, inducing the excision of the t-loops by the SLX1-SLX4 nuclease complex and generating high levels of t-circles (15,18). However, elevated levels of t-circles were not observed in *Rtel1*$^{-/-}$ ES cells (10), and found only in few HHS patients with RTEL1 mutations (5,9), but not in others (7,19,20). In *Rtel1*$^{-/-}$ mouse embryonic and adult fibroblasts, replication fork collapse led to fork reversal that was suggested to be stabilized by telomerase, preventing fork resolution and replication restart (21). Based on these results, telomerase was suggested to play a damaging role and exacerbate the RTEL1-deficiency phenotype, making ES cells particularly susceptible to loss of RTEL1 as they express high levels of telomerase as compared to differentiated cells (21). The multiple reported roles of RTEL1 and the various different phenotypes associated with RTEL1 deficiency failed to reveal what is the main telomeric function of RTEL1 affected in HHS and how do RTEL1 mutations cause telomere shortening and TBD.

To address these questions, we employed fibroblast cell lines derived from two HHS patients carrying different RTEL1 mutations. The first, patient S2 in (7), had compound heterozygous mutations in RTEL1: a nonsense mutation, R974X, and a missense mutation, M492I, located at the center of the helicase domain where other HHS-causing mutations were found (22). The second, patient P5 in (20), had a homozygous V1294F mutation in the C-terminal RING-finger domain, which is present only in the long splice variant reported in the databases. These two cell lines grew poorly in culture, had severely short telomeres and accumulated various telomeric aberrations and DNA damage (20,23). Ectopic expression of hTERT failed to restore telomere length maintenance and to rescue the cells from senescence. However, the ectopic expression of wild-type (WT) RTEL1 in addition to hTERT rescued the cells and suppressed the RTEL1-deficient phenotypes. The use of an inducible (TET-on) promoter to drive RTEL1 expression enabled silencing the ectopic RTEL1 expression and distinguishing the immediate effects of these RTEL1 mutations from phenotypes accumulating over time and secondary effects possibly caused by the severe stress in the primary patient cells. Based on these analyses we suggest that while RTEL1 deficiency causes immediate genome-wide and telomeric damage, this damage is tolerable by the cells and it is the gradual shortening of telomeres that accumulates over time and eventually causes the disease. While rapid telomere deletion by t-loop excision or telomere breakage may contribute in some cell types with some RTEL1 mutations to telomere shortening, the main common cause for this shortening is the inability of telomerase to elongate the telomeres in the absence of a functional RTEL1.

MATERIALS AND METHODS

Cell culture

Informed and written consent was obtained from the patients or their parents (in case of minors). Fibroblasts derived from HHS-patients were grown in DMEM media supplemented with 10% fetal bovine serum, penicillin-streptomycin and 2mM L-glutamine. Twenty percent fetal bovine serum was used for cells that were growing poorly. To induce the ectopic expression of RTEL1, the medium was supplemented with 15 or 30 ng/ml doxycycline (Dox) for P5 and S2 cells, respectively, unless indicated otherwise. To silence its expression, Dox was omitted from the medium and a certified tetracycline-free fetal bovine serum was used. Media and media supplements were purchased from Biological Industries Inc. Beit Haemek, Israel. The rescued S2 cultures shown in Figures 4 and 7, and Supplementary Figures S1, S3D and S4 were grown for ∼60 PDs with Dox before starting these experiments.

Viral vectors, packaging and transduction

Retroviral vectors pWzl-Myc-hPOT1-Hygro and pLPC-Flag-TPP1-Puro (24,25) were a gift from Titia de Lange, Rockefeller University, New York. pBabe-hTERT-GFP (26) was a gift from Sara Selig, Technion, Haifa, Israel. Lentivector pLOX-TERT-iresTK (27) was a gift from Didier Trono (Addgene plasmid #12245; http://n2t.net/addgene:12245; RRID:Addgene_12245). pLenti CMV rtTA3 Blast (w756-1) was a gift from Eric Campeau (Addgene plasmid # 26429; http://n2t.net/addgene:26429; RRID:Addgene_26429). A 3xFLAG tag was added to the RTEL1 variants by PCR amplification and subcloning of the N-terminal fragment of RTEL1 into the AgeI/SgrAI sites in the vectors pLU-H4-TRE-RTEL1v1 (1219aa variant) and pLU-H4-TRE-RTEL1v2 (1300aa variant) generated previously (7), and then subcloning of the FLAG-RTEL1 cDNA into a lentivirus vector under TET-inducible

minimal CMV promotor (pLU-TREmin-puro; a gift of Paul Lieberman, The Wistar Institute, Philadelphia) to generate pGG2F and pGG3F, respectively. The vectors were sequenced to verify the entire 3xFLAG tagged RTEL1 coding sequence. Lentiviral and retroviral particles were produced in the laboratory following standard protocols (28). Fibroblasts were infected twice on consecutive days and three days later selected with 1μg/ml puromycin, 2 μg/ml blasticidin, or 300 μg/ml hygromycin. The medium was replaced every two days until selection was completed. The retroviral vector pBabe-hTERT-GFP was used to infect the S2 fibroblasts, whereas the Lentiviral vector pLOX-TERT-iresTK was used to infect the P5 fibroblasts.

Western Blot

Equal amounts of whole-cell extracts in Laemmli buffer (75mM Tris pH6.8, 2% SDS, 2.5% β-mercaptoethanol, 75 mM DTT, 10% glycerol, Bromophenol blue) were sonicated and electrophoresed on an 8% (w/v) Tris·glycine gel, electroblotted onto a nitrocellulose membrane, probed with the indicated antibodies and visualized by ECL. Antibodies used were: anti-FLAG M2 (A8592) and Anti-GAPDH (G8795) from Sigma-Aldrich, and anti-β-catenin (610153) from BD Transduction Laboratories™.

Genomic DNA extraction

Genomic DNA was extracted following a standard proteinase K-phenol extraction, treated with RNAse A, ethanol precipitated and dissolved in TE.

Southern and in-gel hybridization analyses

Southern blot and in-gel hybridization analyses were done as described (23) except for the telomeric oligonucleotide probe, which was $(AACCCT)_3$. Genomic DNA was digested with HinfI and AluI, unless indicated otherwise and quantified by Qubit fluorometer.

C-circle assay

C-circle assay was performed as described in (29). Briefly, HinfI-digested genomic DNA samples (10, 30 or 100 ng) were incubated in 40 μl reaction mix (0.1 mg/ml BSA, 0.05% Tween, 0.5 mM each dATP, dGTP, dTTP, 1xφ29 DNA polymerase buffer, with and without 7.5 U φ29 DNA polymerase (NEB) overnight at 30°C. The reaction products were run on 0.6% agarose gel in 0.5× TBE for a total of 800 V × h, and the gel was dried and hybridized with a C-rich telomeric probe as above.

T-circle assay

T-circle assay was done following the protocol adapted by Vannier *et al.* for detecting human T-circles (18).

Immunofluorescence

Immunofluorescence was done as described (30), with the following changes. The blocking solution used was 5% BSA in 1× PBS. Primary antibodies used were TRF2 (Novus #NB110-57130), γ-H2AX (Millipore Sigma #05-636). Secondary antibodies were AlexaFluor 594 Donkey anti Rabbit IgG (ThermoFisher #A-21207) and AlexaFluor 488 Goat anti Mouse IgG (ThermoFisher #A-11029). Imaging was performed using a Zeiss LSM 880 with Airyscan microscope or FV-1200 confocal microscope (Olympus, Japan). *ZEN* (Zeiss) and *NIH ImageJ* (http://imagej.nih.gov/ij/) software programs were used for image analysis and foci quantification.

Metaphase telomere FISH

Metaphase spreads were prepared as described (30), and FISH was performed following (31).

qPCR-TRAP assay

Cell pellets were lysed using CHAPS lysis buffer (10 mM Tris HCl pH 7.5, 1 mM $MgCl_2$, 1 mM EGTA, 0.5% CHAPS, 10% glycerol) and telomerase activity was analyzed using a real-time PCR-based semi-quantitative method, as described (16). A duplicated sample that was heat-inactivated at 85°C for 10 min was used as a control. The PCR products were electrophoresed in a 15% acrylamide gel in 1× TBE for 200 V × h and stained with GelStar™, Lonza Inc.

RNA and DNA FISH

FISH was performed as described (32) with the following changes. Cells were permeabilized in CSK buffer (10 mM Pipes pH 7, 100 mM NaCl, 300 mM sucrose, 3 mM $MgCl_2$, 0.5% Triton X-100). Deoxyoligonucleotide probes targeting hTR were: hTR 1 (5′-Cy5-GCTGACATTTTTTGTTTGCTCTAGAATGA ACGGTGGAAGGCGGCAGGCCGAGGCTT), hTR 4 (5′-Cy5-CTCCGTTCCTCTTCCTGCGGCCTGAAAG GCCTGAACCTCGCCCTCGCCCCCGAGAG), hTR 5 (5′-Cy5-ATGTGTGAGCCGAGTCCTGGGTGCACG TCCCACAGCTCAGGGAATCGCGCCGCGCGC), and the telomere deoxyoligonucleotide probe: (5′-TxRd-CCCTAACCCTAACCCTAACCCTAAC CCTAACCCTAA-3′).

Images were collected with an IX-70 microscope (Olympus) and a cooled CCD camera (model CH350; Roper Scientific). Exposure times were the same in duplicated experiments. Image brightness and contrast were adjusted by *Adobe Photoshop* and *NIH ImageJ* (http://imagej.nih.gov/ij/) for display.

Statistical analyses

Statistical analysis was performed using GraphPad Prism 8.0. Two-tailed Student's *t*-test was used and P-value < 0.05 was considered statistically significant.

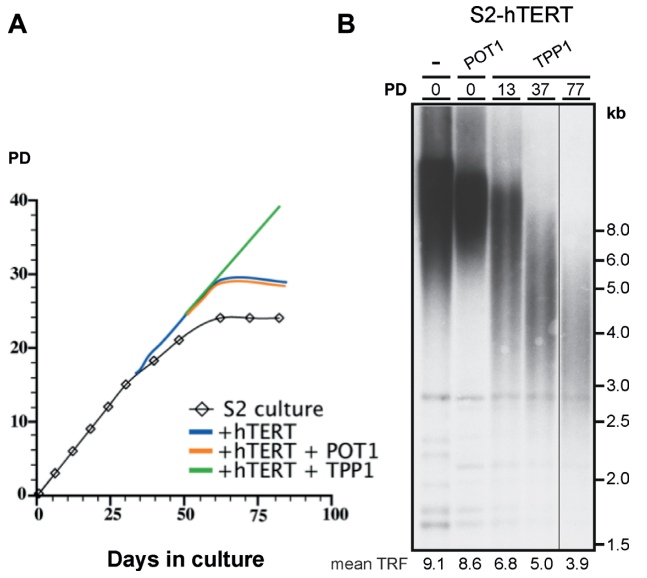

Figure 1. Ectopic expression of TPP1 and hTERT rescued the viability of S2 fibroblasts but failed to maintain telomere length. Primary fibroblasts of patient S2 ($RTEL1_{M492I/R974X}$) (7,23) were grown and transduced with retroviral vectors expressing hTERT and TPP1 or POT1. (**A**) Growth curve of the primary S2 fibroblasts showing cumulative population doublings over time and schematic curves for the indicated transduced cells. (**B**) Southern analysis showing the telomeric restriction fragments (TRF) of the S2-hTERT and S2-hTERT-POT1 soon after passing selection, and S2-hTERT-TPP1 at the indicated PDs. Mean TRF length, measured by *Matelo* (49), is indicated below the lanes.

RESULTS

Ectopic expression of hTERT and TPP1 rescued the S2 patient fibroblasts from early senescence but did not restore telomere length maintenance

We have previously shown that primary fibroblasts derived from an HHS patient S2 carrying compound heterozygous mutations in RTEL1 ($RTEL1_{M492I/R974X}$) are characterized by reduced proliferation rate, diminished telomeric 3′ overhang and the formation of DNA damage foci at telomeres (23). These cells displayed senescence-associated phenotypes such as flattened and enlarged cell morphology and stopped dividing at an early passage. Replicative senescence of primary fibroblasts from healthy donors and some DC patients can be prevented by hTERT expression (33,34). However, initial attempts failed to rescue the S2 patient fibroblasts (23) by transduction with an hTERT-expressing retroviral vector (Figure 1A). The identity of the disease-causing mutation was unknown at the time, but given the diminished telomeric overhang observed in the patient cells we hypothesized that overexpression of TPP1 or POT1, which bind the telomeric overhang as a heterodimer (1), might compensate for the compromised function of the overhang and rescue the cells. TPP1 is crucial for telomerase recruitment, activation and telomere length regulation (35,36) and POT1 binds the telomeric overhang. Indeed, the ectopic expression of TPP1 (but not POT1) in S2 fibroblasts expressing hTERT (S2-hTERT) prevented their rapid senescence and allowed them to grow (Figure 1A). However, their telomeres continued to shorten gradually over 77 population doublings (PDs; Figure 1B; S2-hTERT-TPP1). The 544 amino-acid TPP1 isoform used at the time (now termed TPP1-L) was found recently to be rarely expressed, while a shorter isoform missing 86 amino acids at the N-terminus (TPP1-S) is the main isoform expressed in human cells (37). We confirmed the ectopic expression of TPP1-L in the S2-hTERT cells and found that its mRNA expression level was comparable to that of the endogenous TPP1 (Supplementary Figure S1), presumably due to selection over time in culture for clones expressing low levels of TPP1-L, as observed previously (38). Interestingly, although both isoforms recruit telomerase, only TPP1-S can activate telomere addition (37), which may explain why the rescued cells failed to elongate their telomeres. While we do not understand yet how exactly the ectopic expression of TPP1-L rescued the cells, they provided us with an invaluable opportunity to study the RTEL1 function affected by the mutations in growing cells that are not facing severe stress.

Ectopic expression of RTEL1v2 enabled telomere elongation in the S2-hTERT-TPP1 fibroblasts

Since the S2-hTERT-TPP1 cells grew well but failed to maintain telomere length, this cell line provided an excellent system to test whether ectopic expression of WT RTEL1 would restore telomere maintenance. We have previously shown that RTEL1 variant 2 (1300aa) extended the telomeres of a lymphoblast cell line (LCL) derived from patient S2 (7). However, we observed that the relatively high expression levels of RTEL1 by the histone H4 promoter were toxic in these cells, and were often selected against and silenced. To solve this problem, we established a TET-on system to regulate the expression of the ectopic RTEL1 variants using two lentivectors, one expressing an N-terminal 3XFLAG-tagged RTEL1 (v1 or v2) under six TET responsive elements and a minimal promoter, and another vector expressing the reverse tetracycline trans-activator 3 (rtTA3). To test which of the RTEL1 splice variants can facilitate telomere elongation in the S2-hTERT-TPP1 fibroblasts, we transduced them with vectors expressing rTTA3 and RTEL1v1 or RTEL1v2 (1219aa and 1300aa, respectively), or an empty vector. Another transcript predicted to encode for a 1400aa protein referred to as RTEL1v3 in (7), was later identified as a read-through transcript into the neighboring TNFRSF6B gene that is likely to be degraded by the nonsense-mediated mRNA decay (NMD) pathway (alternative variant RTEL1andTNFRSF6B.aAug10 in the AceView database (39)). The addition of the tetracycline analog doxycycline (Dox) induced the expression of the ectopic RTEL1 while its omission silenced it (Figure 2A). As can be seen in Figure 2C (denatured panel), without ectopic expression of RTEL1 (indicated by '–' above the lanes) or upon expression of RTEL1v1, the S2-hTERT-TPP1 exhibited very short telomeres with mean telomeric restriction fragments (TRF) length below 4 kb. However, RTEL1v2 expression enabled dramatic elongation of telomeres to an average of 6.1 kb. For simplicity, these S2-hTERT-TPP1-RTEL1v2 cells will be termed here 'rescued S2' cells. In addition to the overall telomere length, we estimated the telomeric G-rich 3′ overhang length by first hybridizing the telomeric C-rich probe to the native DNA in the gel to de-

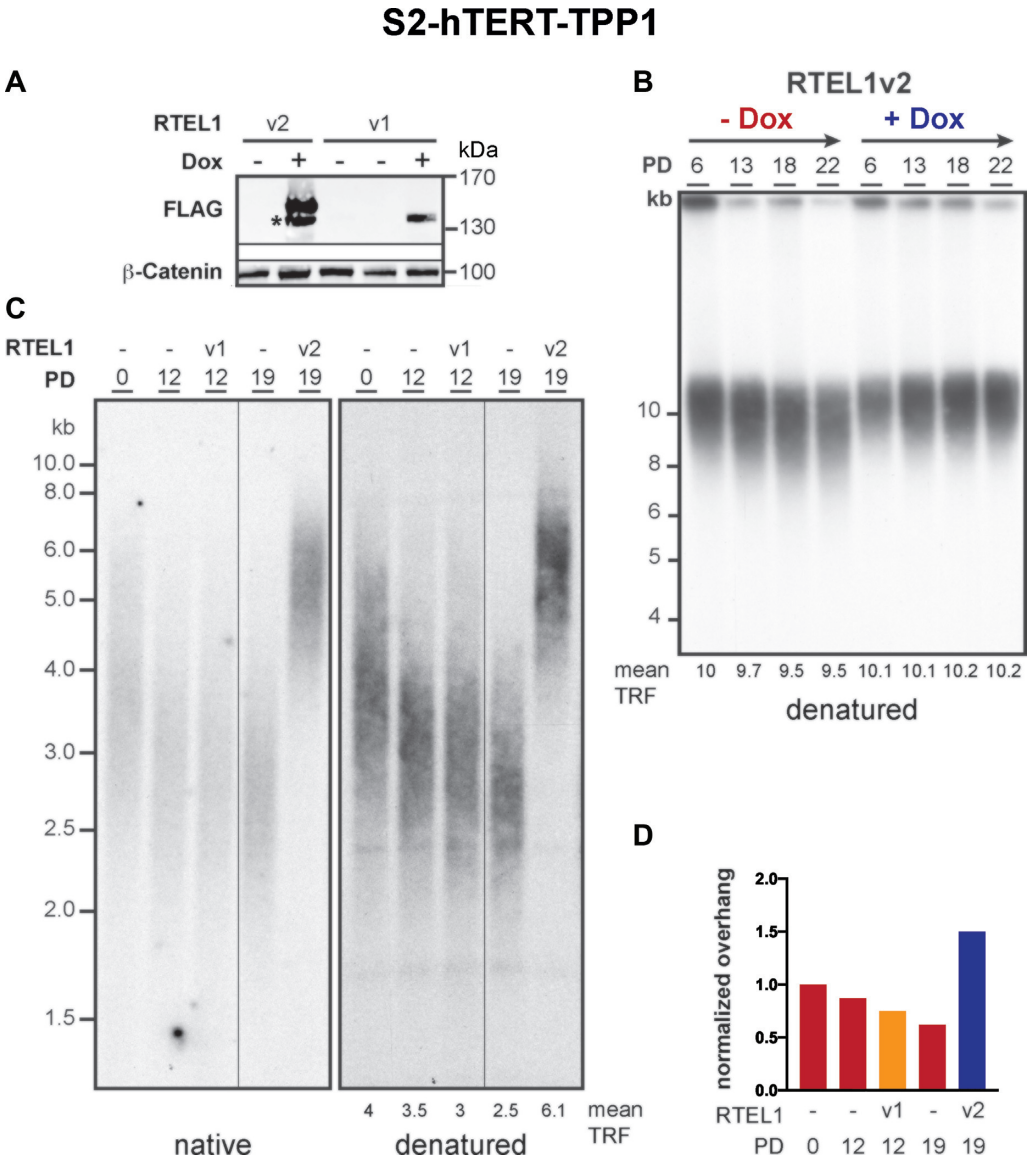

Figure 2. Ectopic expression of RTEL1v2 facilitated telomere elongation in the S2-hTERT-TPP1 fibroblast. (**A**) Western analysis using anti-FLAG antibody to detect FLAG-tagged RTEL1 in S2-hTERT-TPP1 fibroblast transduced with reverse tetracycline trans-activator (rTTA3) and 3xFLAG-RTEL1v1 (1219aa) or 3xFLAG-RTEL1v2 (1300aa) under the a TET inducible promoter, grown in the absence (−) or presence (+) of 60 ng/ml Dox (+), as indicated. A shorter FLAG-tagged protein, presumably generated by proteolysis or premature translation termination of the full length 3xFLAG-RTEL1v2, is indicated by asterisk. β-catenin was used as a loading control. (**B**) An S2-hTERT-TPP1 fibroblast culture expressing RTEL1v2 for 40 PDs (30 ng/ml Dox) was split and half of the culture continued to grow in the presence of Dox while the other half was grown without Dox. Samples were collected in the indicated PDs with and without Dox, genomic DNA was prepared and analyzed by denatured in-gel hybridization. (**C**) Genomic DNA samples of S2-hTERT-TPP1 fibroblasts expressing the indicated RTEL1 variants (or harboring empty vector) were grown in the presence of 30 ng/ml Dox for the indicated PDs and analyzed by in-gel hybridization to the native DNA with a C-rich telomeric probe to detect the signal corresponding to single-stranded telomeric DNA (left panel). After exposure, the DNA was denatured *in situ* and rehybridized to the same probe to reveal all G-rich telomeric DNA (right panel). Mean TRF length, measured by *Matelo* (49), is indicated below the lanes. (**D**) The averaged length of the 3′ overhang was estimated by dividing the native by the denatured hybridization signals and multiplying by the mean telomere length to correct for the bias in signal intensity due to differences in telomere length. The values were normalized to the control (empty vector PD 0), which was set as 1.

tect only single-stranded telomeric DNA (Figure 2C, native panel), and then denaturing and re-hybridizing with the same probe to reveal the total telomeric DNA signal (denatured panel). The relative native/denatured signal was corrected for the bias in signal due to the different telomere length and normalized to the cells at PD 0. Telomere elongation upon the ectopic induction of RTEL1v2 was accompanied by increased native hybridization signal, presumably reflecting an overall 1.5-2 fold elongation of the telomeric 3′ overhang compared to the unrescued cultures (Figure 2D). These observations indicated that RTEL1v2 is needed for both overhang and telomere elongation in these fibroblasts (also see next chapter). Interestingly, in the RTEL1-deficient S2 cells, telomeres shortened gradually, about 50 bp per PD over 64 and 16 PDs (Figures 1B and 2B, respectively), as expected if telomerase action was compromised and unable

to compensate for telomere shortening. However, we cannot rule out the possibility that the ectopic expression of TPP1-L attenuated the shortening to some degree.

RTEL1v2 and hTERT enabled telomere elongation and rescued the P5 fibroblasts

As described above, the 1300aa RTEL1v2, but not the 1219aa RTEL1v1, fully rescued the S2-hTERT-TPP1 fibroblasts and facilitated the elongation of their telomeres (Figure 2B,C). Since the difference between the variants is an 81aa alternative exon at the C-terminus, we hypothesized that this exon (or part of it) is essential for telomere elongation. The C-terminus of the protein was reported to form a metal-coordinating C4C4 RING-finger domain, which is critical for the interaction with TRF2 and the recruitment of RTEL1 to telomeres to unwind the telomere-loops (15). To study this domain of the protein more directly, we obtained cells harboring a homozygous missense mutation substituting a valine residue in position 1294 to phenylalanine, derived from patient P5 in (20). These fibroblasts were transformed by SV40 large T (SV40LT) antigen to facilitate their growth. Nevertheless, they grew poorly in culture and reached senescence quickly, even upon ectopic expression of hTERT (Figure 3C). However, as seen in the rescued S2 cells, the ectopic expression of FLAG-tagged WT RTEL1V2, in addition to hTERT, prevented senescence of the P5-SV40 fibroblasts and fully restored their growth, confirming the importance of RTEL1v2 for cell viability and proliferation (Figure 3B,C). For simplicity, the P5-SV40LT-hTERT-RTEL1v2 cells will be termed here 'rescued P5' cells. Furthermore, telomeres elongated dramatically within ten PDs of induced WT RTEL1v2 expression (Figure 3A, D). As was the case with the rescued S2 cells, turning off the ectopic RTEL1v2 expression by omitting Dox from the medium resulted in gradual telomere shortening while cell growth did not decline over 60 PDs (Figure 3E, denatured panel; and unpublished data). These results demonstrated that similarly to the compound M492I/R974X mutations, the homozygous V1294F mutation in RTEL1 appeared to compromise telomere elongation by telomerase rather than causing large telomere deletions, which would appear as heterogeneous TRF length.

Ten and 15 PDs after omitting Dox (leading to the silencing of the ectopic RTEL1v2), we observed dramatic decline in the native hybridization signal corresponding to the single-stranded G-rich telomeric sequences (Figure 3E,F and Supplementary Figure S2). This decline in the overhang signal is consistent with the diminished G-overhangs observed previously in blood leukocytes, LCLs and primary fibroblasts carrying the M492I and/or R974X mutations (7,23), in patient cells carrying other RTEL1 mutations (40), and upon RTEL1 knockdown (16). ExoI digestion confirmed that the native hybridizations signal corresponds to the single-stranded telomeric 3′-overhang (Supplementary Figure S2C, D). Importantly, upon silencing the ectopic RTEL1v2 expression, the decline in overhang signal occurred while telomeres were still long and no apparent effect on cell viability and proliferation was observed. Thus, the diminished overhang was not a secondary effect of telomere shortening or genotoxic stress but rather a primary consequence of RTEL1 dysfunction, suggesting that RTEL1v2 is essential for the maintenance of the telomeric 3′ overhang.

Telomere-circles are not the main cause for telomere shortening in the RTEL1-deficient patient cells

RTEL1 was reported to function in the resolution of t-loops at S-phase to enable telomere replication (15). Upon the induction of RTEL1 deficiency in mouse embryonic fibroblasts (MEFs), elevated levels of telomere (t)-circles, formed by SLX4-dependent t-loop excision, were observed by a phi29 DNA polymerase-based rolling circle amplification method termed T-circle assay (15,18). However, using two-dimensional (2D) gel electrophoresis no increase in t-circle formation was observed in *mRtel1*$^{-/-}$ mouse ES cells (10). In humans, elevated levels of t-circles were found by the T-circle assay in cells from a few HHS patients (5,9), but not others (19,20). Furthermore, we failed to detect any increase in t-circle formation by 2D gel electrophoresis in LCLs derived from the S2 patient or the heterozygous parents carrying the M492I and R974X mutations (7). These different findings might reflect the different methodology used to measure t-circles, different functions impaired by different point mutations or complete knockout of RTEL1, or different cell types. First, we compared several methods for the detection of t-circles in different human control cells (Supplementary Figure S3). While different conformations of telomeric circles (e.g. T-circles and C-circles) are often defined by the methods designed to detect them, here we define t-circles as any circular telomeric DNA molecule. We used primary fibroblasts, primary fibroblasts expressing ectopic hTERT (Fbr-hTERT), LCLs expressing endogenous hTERT, and U2OS cells, which employ the alternative lengthening of telomeres (ALT) pathway to elongate their telomeres. Human cells expressing telomerase were shown to generate t-circles as a means of trimming and regulating their telomere length (41), while ALT cells were shown to typically generate t-circles with intact C-strand and gapped or nicked G-strand (termed 'C-circles') as part of the recombination based mechanism (29). We used the same four DNA samples in the following assays. The C-circle assay was designed to detect t-circles with an intact C-strand and a nicked or gapped G-strand, which provides a 3′ end to be extended by phi29 DNA polymerase (29) (Supplementary Figure S3A, bottom). Similarly, the reciprocal G-circle assay was designed to detect t-circles with an intact G- and a nicked or gapped C- strands (Supplementary Figure S3A, top). The T-circle assay can detect t-circles with an intact C-strand regardless of the G-strand conformation, because denaturation and annealing of a G-rich telomeric primer provides the 3′ end substrate for the polymerase (18,42) (Supplementary Figure S3C). Finally, the 2D gel electrophoresis can detect any t-circle and distinguish between covalently closed and nicked circles, without the need for amplification (Supplementary Figure S3B). As apparent in Supplementary Figure S3, all methods reliably detected t-circles in U2OS ALT cells. However, the lower levels of t-circles in the LCL and Fbr-hTERT, while clearly detected in 30ng samples by the G- or C-circle assays, required much more DNA (10,000 ng and 1,500 ng for LCL) to be

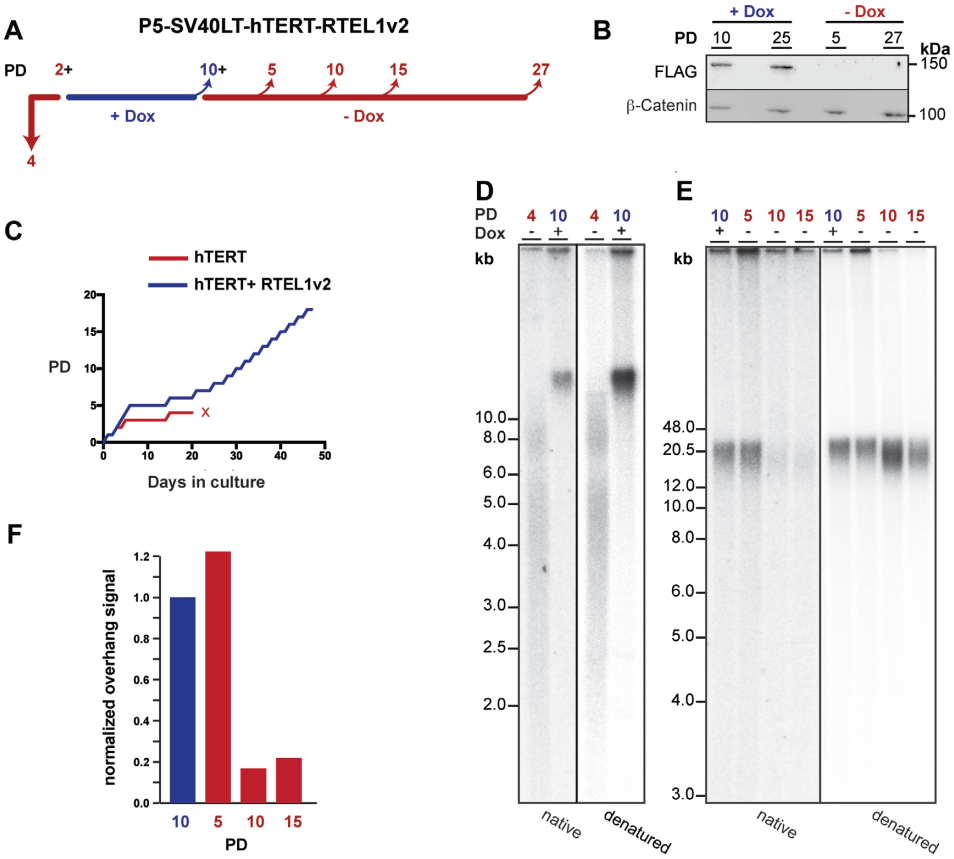

Figure 3. RTEL1v2 enabled telomere elongation and rescued the P5- hTERT fibroblasts. (**A**) P5 fibroblasts carrying a homozygous mutation in RTEL1 ($RTEL1_{V1294F/V1294F}$) were transformed with SV40LT, transduced with hTERT, rTTA3 and 3xFLAG-RTEL1v2 lentivectors and grown for 4 PDs without Dox to reach cell death, or for 2 PDs without Dox, then 10 PDs with 15ng/ml Dox, followed by the indicated PDs without Dox. (**B**) Western analysis showing the expression of 3xFLAG-RTEL1v2 in the presence of Dox and its silencing in the absence of Dox. (**C**) Growth curves of the fibroblasts growing with or without Dox. Red 'X' indicates that the culture stopped growing. (**D**) In-gel hybridization analysis of the cultures grown for 4 PDs without Dox or 10 PDs with Dox, as described in the legend of Figure 2, except that the genomic DNA was cut with HinfI only. (**E**) In-gel hybridization analysis of genomic DNA samples prepared from the culture grown for 10 PDs with Dox and then for the indicated PDs without Dox. Note that this gel was electrophoresed 1.5× longer than the gel in (D). (**F**) Histogram representing the quantified averaged overhang length normalized to the control (PD 10, + Dox).

barely detected by the 2D gel and T-circle assay, respectively, and were not detected at all by 2D gel and T-circle assay in the Fbr-hTERT sample. We concluded that when t-circles are formed in these cells, they provide sufficient substrate to be amplified by the C- and G-circle assays, which were ∼100-fold more sensitive than the T-circle assay or 2D gel.

Next, we employed the sensitive C-circle assay to examine whether t-circle formation was induced upon silencing of WT RTEL1v2 in the patient cells. We detected high levels of t-circles in the control U2OS ALT cells, but not in the rescued P5 fibroblasts, whether expressing WT RTEL1v2 or not (Figure 4A and Supplementary Figure S3D). In the rescued S2 fibroblasts grown without Dox, low levels of t-circles were detected at PD 10 and the levels increased at PD 60 (Figure 4A and Supplementary Figure S3D), but were still significantly lower than in the U2OS cells. Since increased t-circle formation in RTEL1-deficient cells was shown in other publications only by the T-circle assay, we repeated the analysis of the rescued S2 and P5 cells with the same T-circle assay. The results confirmed that only the rescued S2 (but not P5) cells generated low levels of t-circles upon silencing of the WT RTEL1v2, and the levels increased at PD 60 without Dox, but were significantly lower than in U2OS (Figure 4B, C). Altogether comparing various methods for detecting t-circles demonstrated differences in their sensitivity but all of them were reliable in detecting t-circles. Thus, t-circle formation is inherently variable as a function of cell type, telomerase expression and specific RTEL1 mutation. Therefore, t-loop excision cannot explain the telomere shortening observed in all patient cells and the inability of highly expressed telomerase to compensate for this telomere shortening.

Increased genome-wide and telomeric DNA damage response upon induced RTEL1-deficiency in the patient cells

The formation of telomere dysfunction-induced foci (TIFs), typically observed by the formation of γ-H2AX foci colocalizing with telomeres, is considered a hallmark of telomere dysfunction (43). To investigate the effect of the V1294F mutation in RTEL1 on DNA damage we quantified the γ-H2AX foci in interphase nuclei, comparing the rescued P5 cells when expressing WT RTEL1v2 and upon silenc-

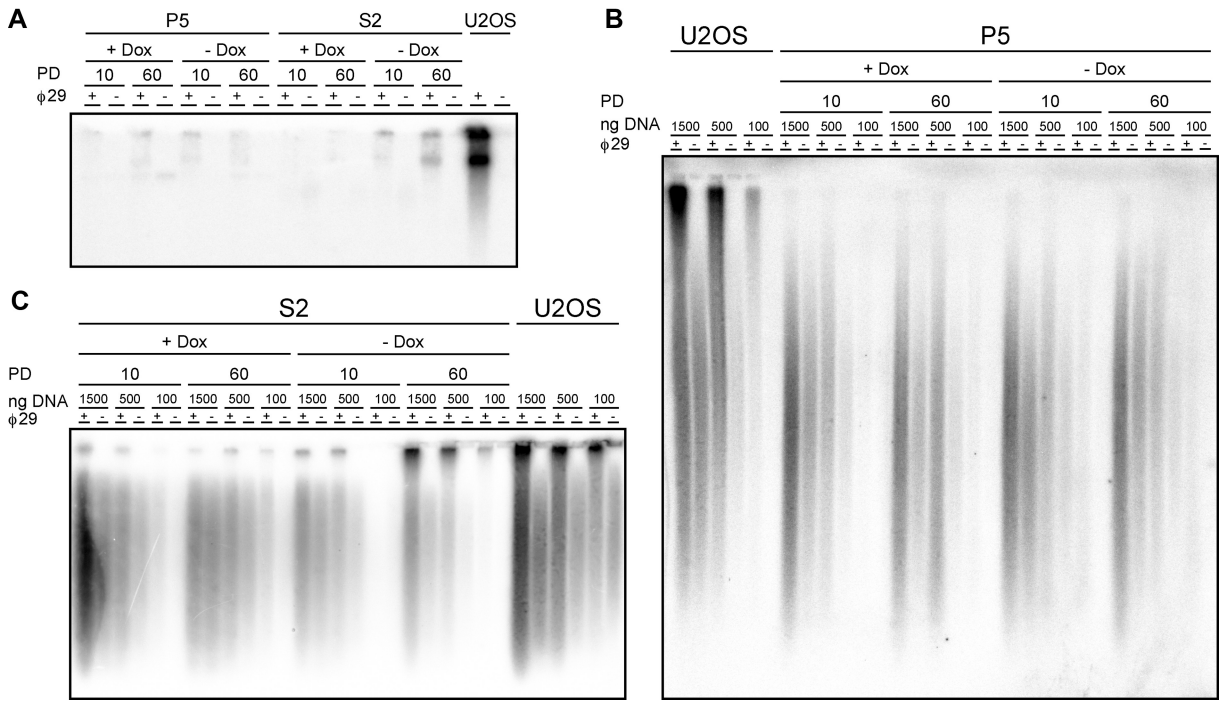

Figure 4. Mild increase in t-circles in the RTEL1-deficient S2 but not in the P5 fibroblasts. Genomic DNA samples freshly-prepared from the rescued P5 and S2 cells grown for 10 or 60 PDs, with or without Dox, and from U2OS ALT cells (as a positive control), were assayed for telomere circles by the C-circle assay using 30 ng DNA samples (**A**), and by the T-circle assay in the indicated amounts of P5 (B) and S2 (C) samples. Note that the gel in the in (**B**) was electrophoresed longer than the gel in (**C**).

ing its expression. The RTEL1-deficient cells, grown 30 PDs without Dox, displayed dramatic increase in the number of γ-H2AX foci (Figure 5A, B). Most of these foci did not colocalize with TRF2, indicating that they were not telomeric. While telomeric γ-H2AX foci were also induced by the RTEL1 deficiency, they constitute only a small fraction of all foci (Figure 5A, C). Overall, the results are consistent with the dual role of RTEL1 in genome-wide and telomere maintenance, and indicate that upon induction of RTEL1-deficiency, DNA damage occurs mostly genome-wide and only a minor fraction of the damage occurs at telomeres. Importantly, the combined telomeric and non-telomeric damage did not significantly affect the growth capacity of these rescued cells, which have long telomeres.

It was reported that RTEL1 deficiency induced replication fork collapse and reversal, and in the absence of RTEL1 the reversed replication forks were stabilized by telomerase and recruited PCNA (21). To examine if RTEL1-deficiency increased the formation of PCNA foci or their association with telomeres in our patient cells, as observed upon induction of conditional knockout of *mRtel1* in MEFs (21), we performed immunofluorescence using anti-PCNA and anti-TRF2 antibodies. No significant increase in the number of PCNA foci or in their localizing to telomeres were observed upon silencing of WT RTEL1v2 in the rescued P5 and S2 cells (Supplementary Figure S4). These results indicated that no significant increase in replication fork stalling or reversal was associated with the RTEL1-deficiency in the examined patient cells.

Increased telomere aberrations upon induced RTEL1-deficiency in the patient cells

To characterize the nature of telomere aberrations that might activate DDR, we examined individual telomeres by FISH performed on metaphase chromosomes of the rescued P5 fibroblasts, comparing the same cells when expressing RTEL1v2, and upon silencing its expression (Figure 6). Immediately upon silencing RTEL1v2 (5 PDs after omitting Dox from the medium), we observed an increase in telomere fragility, and heterogeneity in the telomere signal intensity (Figure 6A, ii and iii). Repeating the assay after further growth in the absence of RTEL1v2 (22 PDs) revealed that only telomeric heterogeneity and loss (Figure 6A, iii and i) accumulated with time, consistent with the role of RTEL1 in telomere length maintenance.

In addition to the telomere aberrations, we noticed the rapid appearance of interstitial telomeric sequences (ITS) five PDs after omitting Dox (Figure 6A, B). Similar insertions were observed in *mRtel1*$^{-/-}$ mouse ES cells and suggested to result from aberrant recombination between a broken internal chromosomal site and a telomere (11). Whether these insertions are generated by replication fork collapse and aberrant recombination (21,44), or by telomerase (45), remains to be studied. Interestingly, these ITS appeared on one chromatid only, indicating that they were detrimental and thus were not inherited or accumulated. The strong negative selection against incorporating ITS could lead to adaptation over time in culture to suppress ITS insertion and decrease their abundance, as observed at the later PD without RTEL1v2 (Figure 6C).

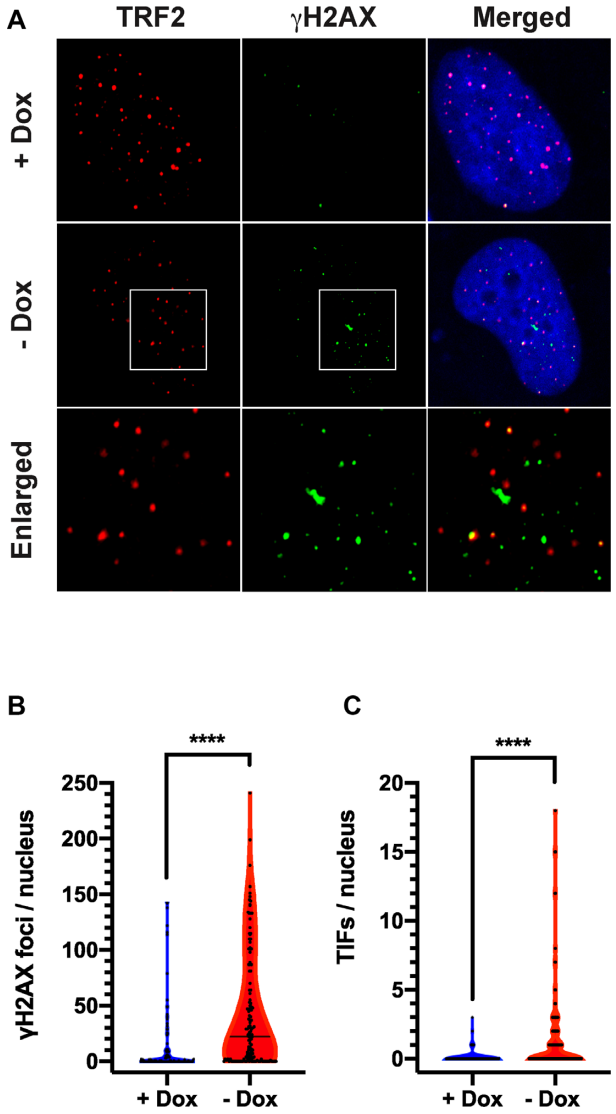

Figure 5. RTEL1-deficient P5 fibroblasts showed increased genome-wide and telomeric DNA damage. The rescued P5 fibroblasts were grown for 10 PDs with Dox to express WT RTEL1v2 and then split and grown for additional 30 PDs with or without Dox and tested for the formation of DDR foci and their colocalization with telomeres. (**A**) Shown are images of interphase nuclei (and enlargements for the '–Dox') stained with DAPI and immunostained for TRF2 (red) and γ-H2AX (green). Violin plots show the numbers of γ-H2AX foci (**B**) and γ-H2AX foci colocalizing with TRF2 (TIFs; **C**) in each nucleus. Data combines two independent experiments; $n = 70$ interphase nuclei per cell line in each experiment. **** Indicate P-values <0.0001 by two-tailed Student's t test.

RTEL1 deficiency did not compromise the *in vitro* activity of telomerase in cell extracts or its recruitment to telomeres

Since the ectopic expression of hTERT in the S2 and P5 patient fibroblasts did not elongate telomeres, we asked if the defect was in the activity of the telomerase catalytic core or in its recruitment to telomeres, as found in other cases of DC and HHS. We found previously that S2 LCL exhibited normal levels of telomerase RNA (hTR) and telomerase *in vitro* activity (23). To examine the *in vitro* telomerase activity in the rescued P5 and S2 fibroblasts we prepared whole cell extracts and assayed them by a real-time PCR-based TRAP assay. We did not find any significant difference in telomerase activity in the patient cells whether expressing or silencing the ectopic RTEL1v2 (Figure 7A), indicating that the RTEL1 mutation did not affect the assembly or *in vitro* activity of the telomerase catalytic core.

Next, we examined the recruitment of telomerase to telomeres by RNA-FISH for hTR, the RNA subunit of telomerase, combined with DNA-FISH for telomeres. The average numbers of hTR foci colocalizing with telomeres in the rescued P5 fibroblasts did not significantly change upon silencing the ectopic RTEL1v2 (Figure 7B,C), suggesting that the recruitment of telomerase to the telomeres was not affected by the V1294F mutation. Altogether, these results indicated normal expression, assembly, catalytic core activity, trafficking and recruitment of telomerase to the telomeres in the RTEL1-deficient patient cells.

DISCUSSION

Mutations causing DC and HHS were found in genes encoding telomerase subunits or factors essential for its processing, assembly, recruitment and action at the telomere, suggesting that the common cause for these diseases is insufficient telomerase action resulting in accelerated telomere shortening (reviewed in (3,4)). However, the way by which RTEL1 mutations cause HHS has been more puzzling since RTEL1 deficiency was reported to cause a broad range of phenotypes, depending on cell type, differentiation status, telomerase expression and the type and position of the RTEL1 mutation (5–21). While in mice, *mRtel1* was discovered as a regulator of telomere elongation and suggested to facilitate telomere extension by telomerase; the mechanism involved is yet unknown (10,11). On the other hand, several publications proposed detailed mechanistic roles for RTEL1, genome wide and at telomeres, such as the resolution of G-quadruplexes to allow replication progression, the resolution of reversed replication forks and replication restart, and the resolution of t-loops (13–15,18,21). Disrupting these roles caused replication defects, DDR activation, telomere fragility and the excision of t-circles, presumably resulting in genomic instability and random and heterogeneous deletions at telomeres. Altogether, while *mRtel1* knockout was suggested to cause telomere shortening in mouse ES cells by hindering telomerase extension of telomeres, other observations in mouse and human cells suggested that RTEL1 deficiency caused telomere shortening by an active process of random telomere deletions. It remained unclear how to reconcile the different observations and how RTEL1 mutations cause telomere shortening and a human disease.

To elucidate the main telomeric function of RTEL1 that is affected in HHS, we used HHS patient cells carrying point mutations, which were pre-selected by their severely short telomeres and their typical HHS clinical symptoms. Unlike RTEL1 knockout, which is lethal, carriers of point mutations were born, albeit developing a fatal disease, and we assumed that these mutations specifically affected the telomeric function of RTEL1. We used two fibroblast cell lines derived from HHS patients: S2, carrying compound heterozygous mutations in RTEL1, M492I and R974X (7) and P5, carrying a homozygous missense mutation in

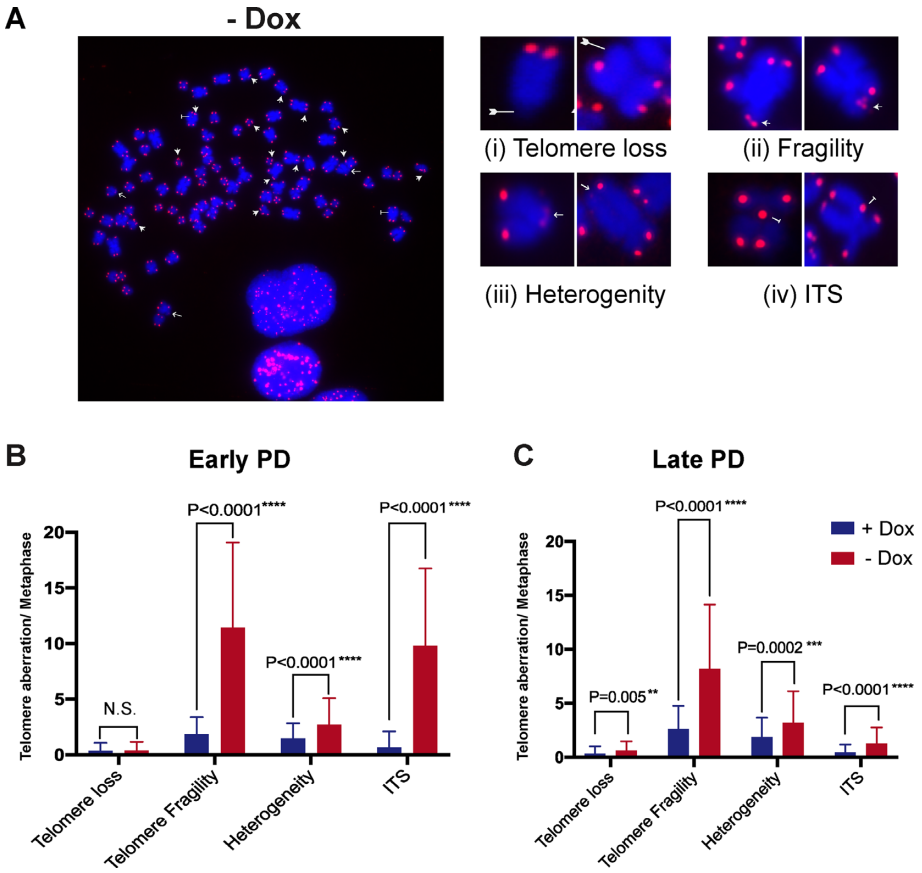

Figure 6. Metaphase chromosomes of RTEL1-deficient P5 fibroblasts displayed increased telomere defects. (**A**) Metaphase nuclei of the rescued P5 fibroblasts were stained with DAPI and hybridized with a telomeric PNA probe. A representative metaphase is shown on the left and various telomere aberrations are shown enlarged on the right: signal-free ends (i), telomere fragility (ii), telomere heterogeneity (iii), and interstitial telomere insertions (ITS; iv). Histograms show the average per metaphase for each type of aberration. (**B**) Early PD cells were grown for 10 PDs with Dox (+ Dox) and then for 5 PDs without Dox (− Dox). (**C**) Late PD cells were grown for 32 PDs with Dox (+ Dox) or 10 PDs with Dox and then 22 PDs without Dox (− Dox). Data are representative of two independent experiments for each early and late PD (mean ± SD; $n = 50$ metaphases). *P*-values were calculated by two-tailed Student's *t* test.

the C-terminus, V1294F (20). Both primary S2 and SV40-transformed P5 fibroblasts grew poorly in culture and displayed progressive telomere shortening and the accumulation of genome-wide and telomeric DNA damage (20,23). The ectopic expression of hTERT and TPP1 (but not POT1) in primary S2 fibroblasts (performed before the RTEL1 mutations were discovered) suppressed their growth defects and enabled them to proliferate for at least 77 PDs, even though average telomere length gradually decreased (Figure 1). This partial suppression of the RTEL1-deficiency phenotype suggested a functional link between the compromised function of RTEL1 and TPP1, which functions in telomerase recruitment, activation and telomere length regulation (35,36). In retrospect, we used a TPP1 isoform (TPP1-L) that is rarely expressed in somatic cells and is compromised in telomere elongation but not in telomerase recruitment (37). Whether the ectopic TPP1-L rescued the cells by increasing the overall amount of TPP1 or by providing a gained function not present in primary cells expressing TPP1-S, is yet to be explored. While primary S2 cells are not available anymore, we believe that ectopic expression of hTERT together with RTEL1 could have rescued them without TPP1, as it rescued the P5 cells.

We established a tunable (TET-on) expression system for WT RTEL1 in these two patient cell lines. Low-level expression of a 1300aa-long splice variant of RTEL1 (RTEL1v2) rapidly elongated the telomeres (Figures 2 and 3), confirming the causal role of the RTEL1 mutations in telomere shortening and the disease. A shorter 1219aa-long variant (RTEL1v1) failed to facilitate telomere elongation, indicating that the C-terminal 81 aa includes an essential element for the telomeric function of RTEL1, consistent with the presence of the HHS-causing V1294F mutation in this C-terminal part of RTEL1v2. Importantly, after rescuing the cells and elongating their telomeres, silencing RTEL1 by omitting Dox from the media caused very slow telomere shortening but did not affect cell growth, indicating that the immediate effects of these RTEL1 mutations are not detrimental, and it is the gradual telomere shortening that causes a progressive disease, likewise other cases of DC and HHS.

We did not see any reduction in the catalytic core telomerase activity in cell extracts prepared from patient cells ((23) and Figure 7A). In addition, the co-localization of telomerase with telomeres was comparable in the presence or absence of ectopic RTEL1v2 (Figure 7B, C), suggesting that although active telomerase had been recruited to the

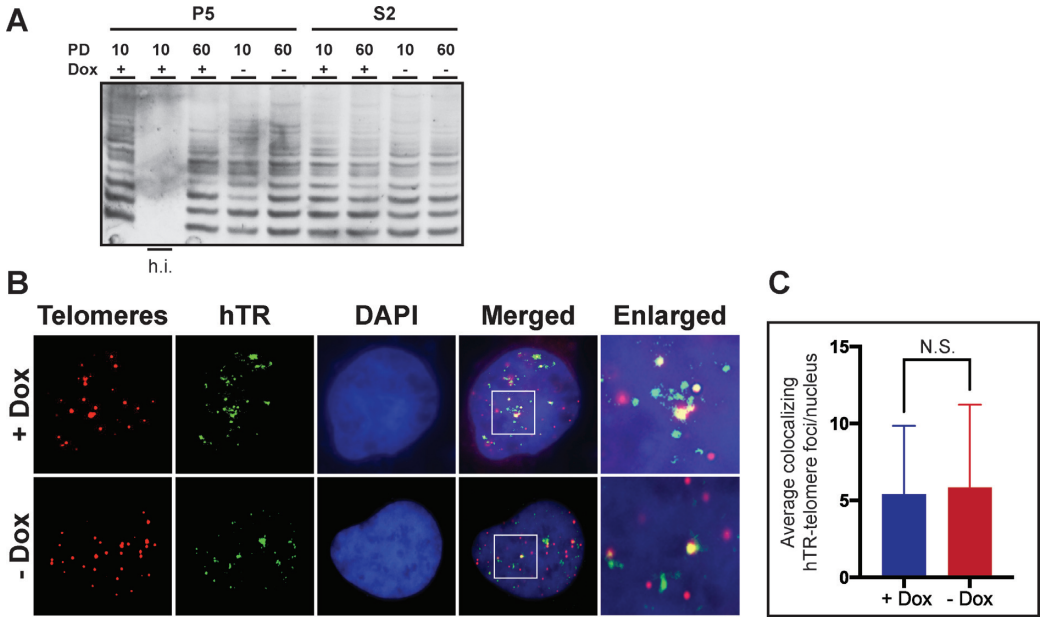

Figure 7. In vitro telomerase activity and recruitment to the telomeres were not compromised in the RTEL1-deficient fibroblasts. (**A**) Polyacrylamide gel electrophoresis of qPCR-TRAP products using 100ng protein extracts from the rescued P5 and S2 cells grown for 10 or 60 PDs with or without Dox. A P5 sample was heat inactivated as a control (indicated by h.i. below the lane). (**B**) The rescued P5 fibroblasts were grown for 10 PDs with Dox to express WT RTEL1v2 (+ Dox) and then split and grown for additional 32 PDs with (+ Dox) or without Dox to silence it (− Dox), and tested by DNA-RNA FISH for telomeres and telomerase RNA (hTR). Representative FISH images of whole nuclei and enlarged telomeres and telomerase foci are shown. (**C**) Histogram showing the average number of colocalizing hTR and telomere foci per nucleus. Data are representative of two independent experiments (mean ± SD; $n =$ 50 interphase nuclei). Two-tailed Student's t test shows no significant difference (ns; P-value = 0.539) in the abundance of colocalizing foci between cells expressing and not expressing RTEL1v2.

telomeres it was unable to elongate the telomeric 3′ end. In addition to the short telomeres, short telomeric overhangs were reported in RTEL1-deficient cells (7,16,23,40). We employed the rescued patient cells to investigate if the short overhangs were generated immediately upon silencing of WT RTEL1v2, or as a secondary effect of the overall telomere shortening or the increased genotoxic stress. The telomeric overhang of the rescued P5 fibroblasts diminished within 10 PDs of omitting Dox from the media and before any significant effect on telomere length was apparent (Figure 3 and Supplementary Figure S2). Since the telomeric 3′ overhang is the substrate for telomerase, diminished overhang may hinder it inaccessible and compromise the ability of telomerase to elongate it. In addition, the 3′ overhang is required for invading a more proximal part of the telomere and base pairing with the C-rich strand to form the protective t-loop structure. Thus, diminished overhang could also result in reduced stability of the t-loops and consequently impaired telomere protection. However, the low frequency of TIF formation (Figure 5) and the lack of significant increase in telomere-telomere fusion upon silencing the ectopic RTEL1 (data not shown) indicated that the telomeres were mostly protected from DNA damage response and repair, arguing against immediate telomere deprotection and suggesting that the higher frequency of TIFs observed in primary cells (23) are due to critically-short telomeres. Altogether, these findings suggest that RTEL1 is involved in the maintenance of the telomeric 3′ overhang, which is required for telomere elongation by telomerase.

Using C-circle and T-circle assays (Figure 4 and Supplementary Figure S3D), we did not detect any increase in t-circles formation in the rescued P5 after RTEL1v2 silencing, excluding the possibility that rapid telomere deletion by t-loop excision is the cause for telomere shortening in these cells. In the rescued S2 cells, however, we observed the accumulation of t-circles over time in culture. While we cannot exclude the possibility that t-loop excision in the form of t-circle contributes to telomere shortening in these S2 fibroblasts, the increase in the levels of t-circles after prolonged growth to PD60 suggests that this is a manifestation of a gradual decrease in telomere stability and function, rather than the direct consequence of RTEL1-deficiency. Furthermore, we have previously examined t-circle formation by 2D gels in LCL derived from the same S2 patient (7). While normal LCLs, expressing endogenous levels of telomerase, generated t-circles (Supplementary Figure S3), in the S2 LCL they were dramatically reduced, as compared with a healthy sibling (Figure 2E in (7)). Additionally, transducing WT LCL and telomerase-positive fibroblasts with lentivectors expressing WT or mutant RTEL1v2 showed that only the WT RTEL1v2 caused an increase in t-circles but not the mutants (Figure 5B and Supplementary Figure S5B in (7)). Altogether these observations are consistent with the notion that t-circle formation can occur in telomerase-positive cells as a form of telomere trimming, or if telomere protection is compromised, but normally telomerase can balance such telomere trimming and maintain stable telomere length, as described previously (41). Furthermore, telomere deletions,

whether caused by t-loop excision or by replication fork collapse and breakage, are expected to activate DDR at telomeres and form TIFs (43). While we observed increased telomere fragility and heterogeneity by FISH upon silencing the ectopic RTEL1v2 in the rescued P5 fibroblasts (Figure 6), they did not accumulate during cell division and the cells proliferated normally. Genome-wide DNA damage was abundant 30 PDs after silencing WT RTEL1v2, but most of the foci did not localize to telomeres (Figure 5), consistent with the proposed role of RTEL1 in genome-wide replication. Telomeric DDR foci (TIFs) also increased upon induction of RTEL1-deficiency, but most of the cells did not show TIFs and only 7% of the cells displayed 5≤ TIFs, confirming that telomere deletion is not the major cause for telomere shortening in the disease.

Altogether, using the inducible expression of WT RTEL1v2 in fibroblasts derived from HHS patients carrying germline mutations in RTEL1, we were able to study the telomeric function of RTEL1, which is impaired in the disease, and particularly to distinguish the immediate response to RTEL1-deficiency from the accumulating damage or secondary effects of the mutations. While the investigated patient cells also show genome-wide damage, this damage is apparently tolerable when telomeres are sufficiently long and in itself does not cause a significant cell growth defects. Dyskerin, PARN and TCAB1/WRAP53β are involved in various pathways other than telomerase action, such as rRNA modification and biogenesis, mRNA stability, DDR and scaRNAs trafficking to the Cajal bodies (46–48). In the context of TBD, however, point mutations in these genes are all associated with the common phenotype of reduced telomerase action. We propose that RTEL1 mutations cause HHS by the same common etiology. While they do not affect the biosynthesis, assembly, localization or catalytic activity of telomerase RNP complexes, they reduce the availability of the telomeric 3′ end to elongation by telomerase, resulting in gradual telomere shortening that eventually activates DDR and leads to cell cycle arrest and loss of cell function.

SUPPLEMENTARY DATA

Supplementary Data are available at NAR Online.

ACKNOWLEDGEMENTS

We are grateful to the patients and families affected by HHS for their generous assistance with samples and information, which made this research possible. We also thank Jan Karlseder and his laboratory members for hosting Aya Awad and helping with methods and advice; Tracy Bryan for the kind gift of fluorescent hTR probes and protocols; and Zhong Deng, Paul Lieberman, Sara Selig and Jennia Michaeli for critical reviewing of the manuscript.

FUNDING

Israel Science Foundation [1729/13, 2071/18, in part]; Israel Cancer Research Fund; Worldwide Cancer Research [15-0338 to Y.T.]; Ministry of Science and Technology, Israel (Navon fellowship to A.A.); Boehringer Ingelheim Fonds (travel grants to A.A., G.G.); INSERM and Ligue Nationale contre le Cancer (Equipe Labellisée La Ligue to P.R.); P.R. is a scientist from Centre National de la Recherche Scientifique (CNRS). Funding for open access charge: Grant money.
Conflict of interest statement. None declared.

REFERENCES

1. de Lange,T. (2018) Shelterin-mediated telomere protection. *Annu. Rev. Genet.*, **52**, 223–247.
2. Maciejowski,J. and de Lange,T. (2017) Telomeres in cancer: tumour suppression and genome instability. *Nat. Rev. Mol. Cell Biol.*, **18**, 175–186.
3. Savage,S.A. (2018) Beginning at the ends: telomeres and human disease. *F1000Res.*, **7**, F1000 Faculty Rev-524.
4. Glousker,G., Touzot,F., Revy,P., Tzfati,Y. and Savage,S.A. (2015) Unraveling the pathogenesis of Hoyeraal-Hreidarsson syndrome, a complex telomere biology disorder. *Br. J. Haematol.*, **170**, 457–471.
5. Ballew,B.J., Joseph,V., De,S., Sarek,G., Vannier,J.B., Stracker,T., Schrader,K.A., Small,T.N., O'Reilly,R., Manschreck,C. *et al.* (2013) A recessive founder mutation in regulator of telomere elongation helicase 1, RTEL1, underlies severe immunodeficiency and features of Hoyeraal Hreidarsson syndrome. *PLos Genet.*, **9**, e1003695.
6. Ballew,B.J., Yeager,M., Jacobs,K., Giri,N., Boland,J., Burdett,L., Alter,B.P. and Savage,S.A. (2013) Germline mutations of regulator of telomere elongation helicase 1, RTEL1, in Dyskeratosis congenita. *Hum. Genet.*, **132**, 473–480.
7. Deng,Z., Glousker,G., Molczan,A., Fox,A.J., Lamm,N., Dheekollu,J., Weizman,O.E., Schertzer,M., Wang,Z., Vladimirova,O. *et al.* (2013) Inherited mutations in the helicase RTEL1 cause telomere dysfunction and Hoyeraal-Hreidarsson syndrome. *Proc. Natl Acad. Sci. U.S.A.*, **110**, E3408–E3416.
8. Le Guen,T., Jullien,L., Touzot,F., Schertzer,M., Gaillard,L., Perderiset,M., Carpentier,W., Nitschke,P., Picard,C., Couillault,G. *et al.* (2013) Human RTEL1 deficiency causes Hoyeraal-Hreidarsson syndrome with short telomeres and genome instability. *Hum. Mol. Genet.*, **22**, 3239–3249.
9. Walne,A.J., Vulliamy,T., Kirwan,M., Plagnol,V. and Dokal,I. (2013) Constitutional mutations in RTEL1 cause severe dyskeratosis congenita. *Am. J. Hum. Genet.*, **92**, 448–453.
10. Uringa,E.J., Lisaingo,K., Pickett,H.A., Brind'amour,J., Rohde,J.H., Zelensky,A., Essers,J. and Lansdorp,P.M. (2012) RTEL1 contributes to DNA replication and repair and telomere maintenance. *Mol. Biol. Cell*, **23**, 2782–2792.
11. Ding,H., Schertzer,M., Wu,X., Gertsenstein,M., Selig,S., Kammori,M., Pourvali,R., Poon,S., Vulto,I., Chavez,E. *et al.* (2004) Regulation of murine telomere length by Rtel: an essential gene encoding a helicase-like protein. *Cell*, **117**, 873–886.
12. Vannier,J.B., Sandhu,S., Petalcorin,M.I., Wu,X., Nabi,Z., Ding,H. and Boulton,S.J. (2013) RTEL1 is a replisome-associated helicase that promotes telomere and genome-wide replication. *Science*, **342**, 239–242.
13. Sfeir,A., Kosiyatrakul,S.T., Hockemeyer,D., MacRae,S.L., Karlseder,J., Schildkraut,C.L. and de Lange,T. (2009) Mammalian telomeres resemble fragile sites and require TRF1 for efficient replication. *Cell*, **138**, 90–103.
14. Sarek,G., Kotsantis,P., Ruis,P., Van Ly,D., Margalef,P., Borel,V., Zheng,X.F., Flynn,H.R., Snijders,A.P., Chowdhury,D. *et al.* (2019) CDK phosphorylation of TRF2 controls t-loop dynamics during the cell cycle. *Nature*, **575**, 523–527.
15. Sarek,G., Vannier,J.B., Panier,S., Petrini,J.H. and Boulton,S.J. (2015) TRF2 recruits RTEL1 to telomeres in S phase to promote t-loop unwinding. *Mol. Cell*, **57**, 622–635.
16. Porreca,R.M., Glousker,G., Awad,A., Matilla Fernandez,M.I., Gibaud,A., Naucke,C., Cohen,S.B., Bryan,T.M., Tzfati,Y., Draskovic,I. *et al.* (2018) Human RTEL1 stabilizes long G-overhangs allowing telomerase-dependent over-extension. *Nucleic Acids Res.*, **46**, 4533–4545.
17. Schertzer,M., Jouravleva,K., Perderiset,M., Dingli,F., Loew,D., Le Guen,T., Bardoni,B., de Villartay,J.P., Revy,P. and Londono-Vallejo,A. (2015) Human regulator of telomere elongation

helicase 1 (RTEL1) is required for the nuclear and cytoplasmic trafficking of pre-U2 RNA. *Nucleic Acids Res.*, **43**, 1834–1847.
18. Vannier,J.B., Pavicic-Kaltenbrunner,V., Petalcorin,M.I., Ding,H. and Boulton,S.J. (2012) RTEL1 dismantles T loops and counteracts telomeric G4-DNA to maintain telomere integrity. *Cell*, **149**, 795–806.
19. Speckmann,C., Sahoo,S.S., Rizzi,M., Hirabayashi,S., Karow,A., Serwas,N.K., Hoemberg,M., Damatova,N., Schindler,D., Vannier,J.B. *et al.* (2017) Clinical and molecular heterogeneity of RTEL1 deficiency. *Front. Immunol.*, **8**, 449.
20. Touzot,F., Kermasson,L., Jullien,L., Moshous,D., Menard,C., Ikinciogullari,A., Dogu,F., Sari,S., Giacobbi-Milet,V., Etzioni,A. *et al.* (2016) Extended clinical and genetic spectrum associated with biallelic RTEL1 mutations. *Blood Adv.*, **1**, 36–46.
21. Margalef,P., Kotsantis,P., Borel,V., Bellelli,R., Panier,S. and Boulton,S.J. (2018) Stabilization of reversed replication forks by telomerase drives telomere catastrophe. *Cell*, **172**, 439–453.
22. Jullien,L., Kannengiesser,C., Kermasson,L., Cormier-Daire,V., Leblanc,T., Soulier,J., Londono-Vallejo,A., de Villartay,J.P., Callebaut,I. and Revy,P. (2016) Mutations of the RTEL1 helicase in a Hoyeraal-Hreidarsson syndrome patient highlight the importance of the ARCH domain. *Hum. Mutat.*, **37**, 469–472.
23. Lamm,N., Ordan,E., Shponkin,R., Richler,C., Aker,M. and Tzfati,Y. (2009) Diminished telomeric 3′ overhangs are associated with telomere dysfunction in Hoyeraal-Hreidarsson syndrome. *PLoS One*, **4**, e5666.
24. Loayza,D. and De Lange,T. (2003) POT1 as a terminal transducer of TRF1 telomere length control. *Nature*, **423**, 1013–1018.
25. Ye,J.Z., Hockemeyer,D., Krutchinsky,A.N., Loayza,D., Hooper,S.M., Chait,B.T. and de Lange,T. (2004) POT1-interacting protein PIP1: a telomere length regulator that recruits POT1 to the TIN2/TRF1 complex. *Genes Dev.*, **18**, 1649–1654.
26. Yalon,M., Gal,S., Segev,Y., Selig,S. and Skorecki,K.L. (2004) Sister chromatid separation at human telomeric regions. *J. Cell Sci.*, **117**, 1961–1970.
27. Salmon,P., Oberholzer,J., Occhiodoro,T., Morel,P., Lou,J. and Trono,D. (2000) Reversible immortalization of human primary cells by lentivector-mediated transfer of specific genes. *Mol. Ther.*, **2**, 404–414.
28. Tiscornia,G., Singer,O. and Verma,I.M. (2006) Production and purification of lentiviral vectors. *Nat. Protoc.*, **1**, 241–245.
29. Henson,J.D., Cao,Y., Huschtscha,L.I., Chang,A.C., Au,A.Y., Pickett,H.A. and Reddel,R.R. (2009) DNA C-circles are specific and quantifiable markers of alternative-lengthening-of-telomeres activity. *Nat. Biotechnol.*, **27**, 1181–1185.
30. Nassour,J., Radford,R., Correia,A., Fuste,J.M., Schoell,B., Jauch,A., Shaw,R.J. and Karlseder,J. (2019) Autophagic cell death restricts chromosomal instability during replicative crisis. *Nature*, **565**, 659–663.
31. Poon,S.S. and Lansdorp,P.M. (2001) Measurements of telomere length on individual chromosomes by image cytometry. *Methods Cell Biol.*, **64**, 69–96.
32. Stern,J.L., Zyner,K.G., Pickett,H.A., Cohen,S.B. and Bryan,T.M. (2012) Telomerase recruitment requires both TCAB1 and Cajal bodies independently. *Mol. Cell. Biol.*, **32**, 2384–2395.
33. Lee,K.M., Choi,K.H. and Ouellette,M.M. (2004) Use of exogenous hTERT to immortalize primary human cells. *Cytotechnology*, **45**, 33–38.
34. Wong,J.M. and Collins,K. (2006) Telomerase RNA level limits telomere maintenance in X-linked dyskeratosis congenita. *Genes Dev.*, **20**, 2848–2858.
35. Sexton,A.N., Regalado,S.G., Lai,C.S., Cost,G.J., O'Neil,C.M., Urnov,F.D., Gregory,P.D., Jaenisch,R., Collins,K. and Hockemeyer,D. (2014) Genetic and molecular identification of three human TPP1 functions in telomerase action: recruitment, activation, and homeostasis set point regulation. *Genes Dev.*, **28**, 1885–1899.
36. Nandakumar,J., Bell,C.F., Weidenfeld,I., Zaug,A.J., Leinwand,L.A. and Cech,T.R. (2012) The TEL patch of telomere protein TPP1 mediates telomerase recruitment and processivity. *Nature*, **492**, 285–289.
37. Grill,S., Bisht,K., Tesmer,V.M., Shami,A.N., Hammoud,S.S. and Nandakumar,J. (2019) Two separation-of-function isoforms of human TPP1 dictate telomerase regulation in somatic and germ cells. *Cell Rep.*, **27**, 3511–3521.
38. Nakashima,M., Nandakumar,J., Sullivan,K.D., Espinosa,J.M. and Cech,T.R. (2013) Inhibition of telomerase recruitment and cancer cell death. *J. Biol. Chem.*, **288**, 33171–33180.
39. Thierry-Mieg,D. and Thierry-Mieg,J. (2006) AceView: a comprehensive cDNA-supported gene and transcripts annotation. *Genome Biol.*, **7**(Suppl. 1), 11–14.
40. Marsh,J.C.W., Gutierrez-Rodrigues,F., Cooper,J., Jiang,J., Gandhi,S., Kajigaya,S., Feng,X., Ibanez,M., Donaires,F.S., Lopes da Silva,J.P. *et al.* (2018) Heterozygous RTEL1 variants in bone marrow failure and myeloid neoplasms. *Blood Adv.*, **2**, 36–48.
41. Pickett,H.A., Cesare,A.J., Johnston,R.L., Neumann,A.A. and Reddel,R.R. (2009) Control of telomere length by a trimming mechanism that involves generation of t-circles. *EMBO J.*, **28**, 799–809.
42. Zellinger,B., Akimcheva,S., Puizina,J., Schirato,M. and Riha,K. (2007) Ku suppresses formation of telomeric circles and alternative telomere lengthening in Arabidopsis. *Mol. Cell*, **27**, 163–169.
43. Takai,H., Smogorzewska,A. and de Lange,T. (2003) DNA damage foci at dysfunctional telomeres. *Curr. Biol.*, **13**, 1549–1556.
44. Uringa,E.J., Youds,J.L., Lisaingo,K., Lansdorp,P.M. and Boulton,S.J. (2011) RTEL1: an essential helicase for telomere maintenance and the regulation of homologous recombination. *Nucleic Acids Res.*, **39**, 1647–1655.
45. Jia,P., Chastain,M., Zou,Y., Her,C. and Chai,W. (2017) Human MLH1 suppresses the insertion of telomeric sequences at intra-chromosomal sites in telomerase-expressing cells. *Nucleic Acids Res.*, **45**, 1219–1232.
46. Benyelles,M., Episkopou,H., O'Donohue,M.F., Kermasson,L., Frange,P., Poulain,F., Burcu Belen,F., Polat,M., Bole-Feysot,C., Langa-Vives,F. *et al.* (2019) Impaired telomere integrity and rRNA biogenesis in PARN-deficient patients and knock-out models. *EMBO Mol. Med.*, **11**, e10201.
47. Henriksson,S. and Farnebo,M. (2015) On the road with WRAP53beta: guardian of Cajal bodies and genome integrity. *Front Genet*, **6**, 91.
48. Yoon,A., Peng,G., Brandenburger,Y., Zollo,O., Xu,W., Rego,E. and Ruggero,D. (2006) Impaired control of IRES-mediated translation in X-linked dyskeratosis congenita. *Science*, **312**, 902–906.
49. Sagie,S., Ellran,E., Katzir,H., Shaked,R., Yehezkel,S., Laevsky,I., Ghanayim,A., Geiger,D., Tzukerman,M. and Selig,S. (2014) Induced pluripotent stem cells as a model for telomeric abnormalities in ICF type I syndrome. *Hum. Mol. Genet.*, **23**, 3629–3640.